AIMS Mathematics, 9(4): 9989–10009.
DOI: 10.3934/math.2024489
Received: 04 January 2024
Revised: 15 February 2024
Accepted: 04 March 2024
Published: 13 March 2024

http://www.aimspress.com/journal/Math

Research article

Model-free scheme using time delay estimation with fixed-time FSMC for the nonlinear robot dynamics

Saim Ahmed[1,2,*], **Ahmad Taher Azar**[1,2,3] **and Ibraheem Kasim Ibraheem**[4,5]

[1] College of Computer and Information Sciences, Prince Sultan University, Riyadh 11586, Saudi Arabia; Emails: ahmad_t_azar@ieee.org, aazar@psu.edu.sa

[2] Automated Systems and Soft Computing Lab (ASSCL), Prince Sultan University, Riyadh 11586, Saudi Arabia

[3] Faculty of Computers and Artificial Intelligence, Benha University, Benha 13518, Egypt; Email: ahmad.azar@fci.bu.edu.eg

[4] Department of Electrical Engineering, College of Engineering, University of Baghdad, Baghdad 10001, Iraq; Email: ibraheemki@coeng.uobaghdad.edu.iq

[5] Department of Electronics and Communication Engineering, Uruk University, Baghdad 10001, Iraq

* **Correspondence:** Email: sahmed@psu.edu.sa.

Abstract: This paper presents a scheme of time-delay estimation (TDE) for unknown nonlinear robotic systems with uncertainty and external disturbances that utilizes fractional-order fixed-time sliding mode control (TDEFxFSMC). First, a detailed explanation and design concept of fractional-order fixed-time sliding mode control (FxFSMC) are provided. High performance tracking positions, non-chatter control inputs, and nonsingular fixed-time control are all realized with the FxSMC method. The proposed approach performs better and obtains superior performance when FxSMC is paired with fractional-order control. Furthermore, a TDE scheme is included in the suggested strategy to estimate the unknown nonlinear dynamics. Afterward, the suggested system's capacity to reach stability in fixed time is determined by using Lyapunov analyses. By showing the outcomes of the proposed technique applied to nonlinear robot dynamics, the efficacy of the recommended method is assessed, illustrated, and compared with the existing control scheme.

Keywords: time delay estimation; fractional-order control; fixed-time sliding mode control; nonlinear robotic system
Mathematics Subject Classification: 93C10, 93C40, 93D09, 93D21, 93B52

1. Introduction

Applications of control engineering are typically used in nonlinear systems under the conditions of unknown dynamics and external perturbations. Because robotic systems are nonlinear by nature, estimating their dynamics is a difficult task. Robot manipulators [1], mobile robots [2], crane systems [3], powered wheelchairs [4], and unmanned aerial vehicles [5] are a few examples of these systems. These systems frequently encounter a variety of uncertainties and disturbances, all of which may have an effect on the system's overall performance and stability [6]. Scholars devised various control schemes, including the sliding mode control (SMC) method [7], to tackle and resolve these issues.

Control schemes based on models, like SMC, are frequently utilized. Since the SMC approach can effectively handle uncertainties and disturbances, it has been broadly utilized in the field of nonlinear controllers, increasing the robustness of the system. Nevertheless, a major obstacle to this strategy's implementation is its slow convergence and excessive chatter of the control input [8, 9]. Chattering occasionally causes inadvertent disruptions to the system, which may disrupt its functionality. Over time, advances in SMC have been made to address these issues, including terminal SMC, fast nonsingular SMC, and finite-time SMC [10–14]. On the other hand, in the case of the finite-time approach, the convergence is highly dependent on the initial states. Thus, a fixed-time control strategy provides an alternative to figuring out the convergence period, irrespective of the initial conditions [15].

The finite-time SMC challenge has been resolved through the use of fixed-time SMC. Fixed-time SMC is helpful for uncertain dynamical systems because the system can approach convergence in a set amount of time. Leading researchers have recently emphasized their interest in studying this specific topic. Some scholars suggest using fixed-time SMC to more effectively handle the uncertainties and disturbances present in a nonlinear system [16]. In the realm of advanced research on uncertain perturbed dynamics of autonomous underwater vehicles under actuator faults and input saturation, a neural network with fixed-time SMC approach has been devised [17]. Furthermore, a fractional-order chaotic system was successfully managed and brought under control by using a fixed-time SMC scheme [18].

One area of mathematics that has been around since the 17th century is fractional-order calculus. The broader application of integer-order calculus to non-integer order is known as fractional-order calculus [19, 20]. Researchers have become interested in the use of fractional calculus in science and engineering in the last few decades [21, 22]. Numerous fractional-order based control schemes, such as fractional-order PID controller, fractional-order SMC (FSMC), and fractional optimal controllers, have been proposed because it offers better flexibility to enhance control performance and efficiency of the closed-loop system [23–25]. FSMC was developed for application in many different research areas, such as robotic arm systems [26], multimachine power systems [27], supercavitating underwater vehicles [28], tethered satellites [29], fractional-order chaotic systems [30], permanent magnet synchronous generator wind turbines [31], and so forth. Moreover, a fractional-order scheme has been implemented with the fixed SMC for the application of nonlinear robotic dynamics [6, 7].

Because the nonlinear elements in the dynamical equations require the computation of the entire dynamic system, controllers based on robot dynamical models, such as computed torque control and optimal control, are generally utilized [32, 33]. Additionally, intelligent control schemes have been employed as model-free methods; although they are robust as well as adaptive, there are disadvantages

to their use, particularly, they require very sophisticated and lengthy training to fine-tune several aspects that significantly affect control performance [34]. Consequently, because of their complexity, neither intelligent nor model-based approaches are appropriate for broad application.

The time-delay estimation (TDE) method is a simple replacement for the previously described techniques [35]. If a controller has a sufficiently short sampling period, the TDE uses time-delayed state variables and control input to estimate the current dynamics of the system. Time-delay control (TDC) is a well-known technique that was introduced by Toumi and Ito [35], and Hsia and Gao [36]. It involves using the delayed estimated dynamics to cancel out nonlinear dynamics. Despite its simple form, the TDC scheme is numerically efficient, model-free, and resilient. Therefore, TDE combined with SMC can be utilized to simultaneously offer control, estimation, and robustness for unknown uncertain nonlinear dynamics [37]. To the best of the authors' knowledge, no literature on the TDE with fractional fixed-time SMC scheme for robotic systems, as realized under the new fixed-time lemma, has been developed.

This paper presents a model-free approach based on TDE with fractional-order fixed-time sliding mode control (TDEFxFSMC) to control the unknown robotic manipulator systems under constrained external disturbances. The main contributions of the proposed scheme are given below:

(1) The primary goals were to estimate the unknown nonlinear dynamics, improve tracking, and achieve robustness against uncertainties of the closed-loop system.
(2) TDE has been used to estimate the unknown uncertain robotic manipulator dynamics under external disturbances.
(3) A fractional SMC scheme has been designed to realize better tracking, convergence and transient performances in fixed time.
(4) The stability analyses for the error and sliding manifold have been established by using the Lyapunov approach.

This study is organized as follows. Section 2 discusses system modeling, TDE, and control design in detail. The Lyapunov theorem is introduced in Section 3 to provide fixed-time stability. Section 4 provides numerical simulations of the proposed scheme. A discussion of the findings is presented in Section 5. In the end, this work is concluded in Section 6.

2. TDE based scheme using fixed-time FSMC

This section begins with a study of TDE with a fixed-time fractional-order sliding surface and nonlinear dynamical system. Next, in order to provide TDEFxFSMC for unknown dynamical systems, a mechanism for proposed control is constructed. Consequently, the nonlinear system is described by using the robot manipulator dynamics given by [12]

$$\mathfrak{m}(q)\ddot{q} + \mathfrak{c}(q,\dot{q})\dot{q} + \mathfrak{g}(q) + \mathfrak{f}(t) + \mathfrak{d}(t) = \mathfrak{u} \tag{2.1}$$

where q, $\dot{q}$, and $\ddot{q}$ are the angular position, angular velocity, and angular acceleration, respectively. $\mathfrak{m}(q) \in \mathbb{R}^{n\times n}$ is the positive definite inertia matrix with $0 < \mathfrak{m}_{min} \leq \|\mathfrak{m}(q)\| \leq \mathfrak{m}_{max}$, where $\mathfrak{m}_{min}$ and $\mathfrak{m}_{max}$ are the eigenvalues of $\mathfrak{m}(q)$. $\mathfrak{c}(q,\dot{q}) \in \mathbb{R}^{n\times n}$ denotes the coriolis and centripetal forces, $\mathfrak{g}(q) \in \mathbb{R}^n$ represents the gravitational force, $\mathfrak{f}(t) \in \mathbb{R}^n$ and $\mathfrak{d}(t) \in \mathbb{R}^n$ express the uncertainty and unknown external disturbances, respectively, and $\mathfrak{u} \in \mathbb{R}^n$ denotes the control torque.

The equation given in (2.1) can be rewritten as

$$\begin{aligned} &\alpha\ddot{q} + \left[\mathfrak{m}(q)\ddot{q} - \alpha\ddot{q} + \mathfrak{c}(q,\dot{q})\dot{q} + \mathfrak{g}(q) + \mathfrak{f}(t) + \mathfrak{d}(t)\right] = \mathfrak{u} \\ &\Rightarrow \ddot{q} + \alpha^{-1}\left[\mathfrak{m}(q)\ddot{q} - \alpha\ddot{q} + \mathfrak{c}(q,\dot{q})\dot{q} + \mathfrak{g}(q) + \mathfrak{f}(t) + \mathfrak{d}(t)\right] = \alpha^{-1}\mathfrak{u}. \end{aligned} \tag{2.2}$$

For the application of TDE, the following expression is given

$$\ddot{q} = \alpha^{-1}\mathfrak{u} + \mathfrak{Y}(q,\dot{q},\ddot{q}) \tag{2.3}$$

where $\alpha > 0$ and

$$\mathfrak{Y}(q,\dot{q},\ddot{q}) = -\alpha^{-1}\left[\mathfrak{m}(q)\ddot{q} - \alpha\ddot{q} + \mathfrak{c}(q,\dot{q})\dot{q} + \mathfrak{g}(q) + \mathfrak{f}(t) + \mathfrak{d}\,(t)\right]$$

denotes the unknown uncertain robot manipulator dynamics with disturbance.

The tracking error can be obtained as follows:

$$\ddot{\varepsilon} = \alpha^{-1}\mathfrak{u} + \mathfrak{Y}(q,\dot{q},\ddot{q}) - \ddot{q}_d \tag{2.4}$$

with $\varepsilon = q - q_d$ and q_d is the desired angular position.

2.1. Fractional-order fixed-time sliding manifold

The purpose of sliding surface construction is to provide nonsingularity and obtain the benefits of fractional-order and fixed-time SMC. The recommended fixed-time surface is applied to offer precise and rapid control performance for the robot's uncertain dynamics. Thus, the following sliding surface design is provided:

$$\mathcal{S} = \mathcal{D}^{\gamma}e + \mathcal{K}_1\mathcal{D}^{\gamma-1}\left[|e|^{\lambda_1}sign(e)\right] + \mathcal{K}_2\mathcal{D}^{\gamma-1}\left[|e|^{\lambda_2}sign(e)\right] \tag{2.5}$$

where $e = \dot{\varepsilon} + \kappa_1|\varepsilon|^{\varsigma_1}sign(\varepsilon) + \kappa_2|\varepsilon|^{\varsigma_2}sign(\varepsilon)$, $\mathcal{S}$ is the sliding surface, and κ_1, κ_2, $\mathcal{K}_1$, $\mathcal{K}_2 > 0$ are known constants. The constants of the exponent are $0 < \lambda_1 < 1$, $\lambda_2 > 1$, $0 < \varsigma_1 < 1$ and $\varsigma_2 > 1$. Additionally, γ is a fractional-order value with the range (0,1), and $\mathcal{D}^{\gamma}$ is the fractional derivative.

Equation (2.5) can be derived as follows:

$$\dot{\mathcal{S}} = \mathcal{D}^{\gamma}\dot{e} + \mathcal{K}_1\mathcal{D}^{\gamma}\left[|e|^{\lambda_1}sign(e)\right] + \mathcal{K}_2\mathcal{D}^{\gamma}\left[|e|^{\lambda_2}sign(e)\right]. \tag{2.6}$$

Substitution of $\dot{e}$ in (2.6) yields

$$\dot{\mathcal{S}} = \mathcal{D}^{\gamma}\left[\ddot{\varepsilon} + \kappa_1\varsigma_1|\varepsilon|^{\varsigma_1-1}\dot{\varepsilon} + \kappa_2\varsigma_2|\varepsilon|^{\varsigma_2-1}\dot{\varepsilon}\right] + \mathcal{K}_1\mathcal{D}^{\gamma}\left[|e|^{\lambda_1}sign(e)\right] + \mathcal{K}_2\mathcal{D}^{\gamma}\left[|e|^{\lambda_2}sign(e)\right]. \tag{2.7}$$

Substitution of (2.4) into (2.7) yields

$$\begin{aligned} \dot{\mathcal{S}} = {} & \mathcal{D}^{\gamma}\left[\alpha^{-1}\mathfrak{u} + \mathfrak{Y}(q,\dot{q},\ddot{q}) - \ddot{q}_d + \kappa_1\varsigma_1|\varepsilon|^{\varsigma_1-1}\dot{\varepsilon} + \kappa_2\varsigma_2|\varepsilon|^{\varsigma_2-1}\dot{\varepsilon}\right] \\ & + \mathcal{K}_1\mathcal{D}^{\gamma}\left[|e|^{\lambda_1}sign(e)\right] + \mathcal{K}_2\mathcal{D}^{\gamma}\left[|e|^{\lambda_2}sign(e)\right]. \end{aligned} \tag{2.8}$$

Note that

$$|e|^{\lambda_i}sign(e) = \left[|e_1|^{\lambda_i}sign(e_1),\ |e_2|^{\lambda_i}sign(e_2), ..., |e_n|^{\lambda_i}sign(e_n)\right]^T$$

and

$$|\varepsilon|^{\varsigma_i-1} = diag\left(|\varepsilon_1|^{\varsigma_i-1},\ |\varepsilon_2|^{\varsigma_i-1}, ...,\ |\varepsilon_n|^{\varsigma_i-1}\right).$$

Now, the suggested model-free control method based on TDEFxFSMC for the unknown dynamical robot system will be designed. Achieving strong tracking performance and model-free control will be the goal of this.

2.2. Design of TDEFxFSMC scheme

In order to control the unknown nonlinear robot dynamics in the presence of unknown disturbances, the TDEFxFSMC approach is presented as

$$\mathfrak{u} = \mathfrak{u}_n + \mathfrak{u}_e \tag{2.9}$$

where $\mathfrak{u}_n$ is the nominal control input and $\mathfrak{u}_e$ is the estimation of the unknown uncertain dynamics via TDE.

$$\mathfrak{u}_n = -\alpha \begin{pmatrix} -\ddot{q}_d + \kappa_1 \varsigma_1 |\varepsilon|^{\varsigma_1 - 1} \dot{\varepsilon} + \kappa_2 \varsigma_2 |\varepsilon|^{\varsigma_2 - 1} \dot{\varepsilon} \\ +\mathcal{K}_1 \left[|e|^{\lambda_1} sign(e) \right] + \mathcal{K}_2 \left[|e|^{\lambda_2} sign(e) \right] \end{pmatrix} \tag{2.10}$$

and

$$\mathfrak{u}_e = -\alpha \left(\hat{\mathfrak{Y}}(q, \dot{q}, \ddot{q}) + \bar{\mathcal{K}}_1 \mathcal{D}^{-\gamma} \left[|\mathcal{S}|^{\mu_1} sign(\mathcal{S}) \right] + \bar{\mathcal{K}}_2 \mathcal{D}^{-\gamma} \left[|\mathcal{S}|^{\mu_2} sign(\mathcal{S}) \right] \right) \tag{2.11}$$

where $|\varepsilon|^{\varsigma_1 - 1} = 0$ if $\varepsilon = 0$, and $\bar{\mathcal{K}}_1 > 0$, $\bar{\mathcal{K}}_2 > 0$, $0 < \mu_1 < 1$, $\mu_2 > 1$ are known constants.

Proposed controller (2.9) is substituted in (2.8) to obtain

$$\begin{aligned} \dot{\mathcal{S}} = \mathcal{D}^{\gamma} \Bigg[& \alpha^{-1} \left\{ \begin{array}{l} -\alpha \begin{pmatrix} -\ddot{q}_d + \kappa_1 \varsigma_1 |\varepsilon|^{\varsigma_1 - 1} \dot{\varepsilon} + \kappa_2 \varsigma_2 |\varepsilon|^{\varsigma_2 - 1} \dot{\varepsilon} \\ +\mathcal{K}_1 \left[|e|^{\lambda_1} sign(e) \right] + \mathcal{K}_2 \left[|e|^{\lambda_2} sign(e) \right] \end{pmatrix} \\ -\alpha \left(\hat{\mathfrak{Y}}(q, \dot{q}, \ddot{q}) + \bar{\mathcal{K}}_1 \mathcal{D}^{-\gamma} \left[|\mathcal{S}|^{\mu_1} sign(\mathcal{S}) \right] + \bar{\mathcal{K}}_2 \mathcal{D}^{-\gamma} \left[|\mathcal{S}|^{\mu_2} sign(\mathcal{S}) \right] \right) \end{array} \right\} \\ & + \mathfrak{Y}(q, \dot{q}, \ddot{q}) - \ddot{q}_d + \kappa_1 \varsigma_1 |\varepsilon|^{\varsigma_1 - 1} \dot{\varepsilon} + \kappa_2 \varsigma_2 |\varepsilon|^{\varsigma_2 - 1} \dot{\varepsilon} \Bigg] \\ & + \mathcal{K}_1 \mathcal{D}^{\gamma} \left[|e|^{\lambda_1} sign(e) \right] + \mathcal{K}_2 \mathcal{D}^{\gamma} \left[|e|^{\lambda_2} sign(e) \right]. \end{aligned} \tag{2.12}$$

By solving (2.12), one can obtain

$$\dot{\mathcal{S}} = \mathcal{D}^{\gamma} F - \bar{\mathcal{K}}_1 \left[|\mathcal{S}|^{\mu_1} sgn(\mathcal{S}) \right] - \bar{\mathcal{K}}_2 \left[|\mathcal{S}|^{\mu_2} sgn(\mathcal{S}) \right] \tag{2.13}$$

where $F = \mathfrak{Y}(q, \dot{q}, \ddot{q}) - \hat{\mathfrak{Y}}(q, \dot{q}, \ddot{q})$ and $\hat{\mathfrak{Y}}(q, \dot{q}, \ddot{q})$ represents the estimated dynamics obtained by using the time delayed form of (2.3); thus, one can take into account the constant time delay z as follows:

$$\hat{\mathfrak{Y}}(q, \dot{q}, \ddot{q}) = \mathfrak{Y}(q, \dot{q}, \ddot{q})_{(t-z)} = \ddot{q}_{(t-z)} - \alpha^{-1} \mathfrak{u}_{(t-z)}. \tag{2.14}$$

Assumption 1. The bounded TDE error inequality can be expressed as follows:

$$\mathcal{D}^{\gamma} F \leq \Xi \tag{2.15}$$

where $\Xi > 0$ is constant.

The unknown system dynamics, uncertainty, and external disturbances will be estimated by using TDE dynamics (2.14), and fractional-order fixed-time SMC enhances the position tracking and control performances. Thus, the TDEFxFSMC approach effectively tracks the desired performance of the uncertain robotic system and provides the model-free scheme for the unknown robot dynamics. Figure 1 depicts the comprehensive model of the suggested technique. The fixed-time stability of the proposed system will be analyzed in the following section.

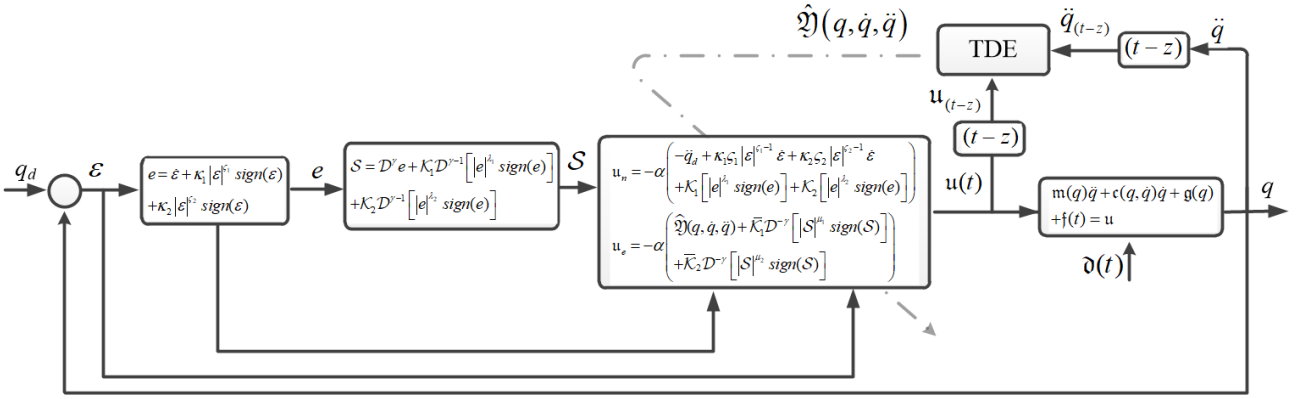

Figure 1. Proposed scheme diagram.

3. Stability analysis

By executing the necessary calculations through the use of Lyapunov analysis, this section details how to determine the overall stability of the system. The following lemmas are important and will be applied for the proof of stability analyses.

Lemma 1. Suppose that the appropriate continuous Lyapunov function, $\mathcal{V}$, is available such that [38]

$$\dot{\mathcal{V}} \leq -h_1\mathcal{V}^{p_1} - h_2\mathcal{V}^{p_2} + r \tag{3.1}$$

where h_1, $h_2 > 0$, $0 < p_1 < 1$ $p_2 > 1$ and $0 < r < \infty$. Thus, the overall dynamics are said to be fixed-time stable, and the region of convergence is determined by

$$\mathcal{V} \leq \min\left\{\left(\frac{r}{h_1(1-\varpi)}\right)^{\frac{1}{p_1}}, \left(\frac{r}{h_2(1-\varpi)}\right)^{\frac{1}{p_2}}\right\} \tag{3.2}$$

where $0 < \varpi < 1$. And the settling time T can be computed as follows:

$$T \leq \frac{1}{h_1\varpi(1-p_1)} + \frac{1}{h_2\varpi(p_2-1)}. \tag{3.3}$$

Lemma 2. For the system $\dot{y}(x) = f(x,y)$, $y(0) = y_0$, taking into account the system's fixed-time convergence stability, the Lyapunov function $\mathcal{V}(y)$ satisfies the following conditions [39, 40]:
i. $\mathcal{V}(y) = 0 \Leftrightarrow y = 0$,
ii. $\dot{\mathcal{V}}(y) \leq -h_1\mathcal{V}^{p_1}(y) - h_2\mathcal{V}(y)^{p_2}$ for $h_1, h_2 > 0$, $0 < p_1 < 1$ and $p_2 > 1$. Thus, the settling time T can be computed as follows:

$$T \leq \frac{1}{h_1(1-p_1)} + \frac{1}{h_2(p_2-1)}. \tag{3.4}$$

Lemma 3. The inequalities are given for ϕ_i [15]

$$\begin{aligned} &\sum_{i=1}^{n} |\phi_i|^{1+\varphi} \geq \left(\sum_{i=1}^{n} |\phi_i|^2 \right)^{\frac{1+\varphi}{2}}, \ if \ 0 < \varphi < 1, \\ &\sum_{i=1}^{n} |\phi_i|^{\varphi} \geq n^{1-\varphi} \left(\sum_{i=1}^{n} |\phi_i| \right)^{\varphi}, \ if \ \varphi > 1. \end{aligned} \tag{3.5}$$

Theorem 1. The proposed sliding surface (2.5), combined with the TDEFxFSMC method (2.9) for the unknown robotic manipulator system (2.1) under uncertainties and external disturbances, will cause the states of the dynamical system to converge in a fixed time.

Proof. The Lyapunov functional candidate $\mathcal{V}_1$ is given as

$$\mathcal{V}_1 = \frac{1}{2} \sum_{i=1}^{n} \mathcal{S}_i^2. \tag{3.6}$$

The time derivative of (3.6) is given as

$$\dot{\mathcal{V}}_1 = \sum_{i=1}^{n} \mathcal{S}_i \dot{\mathcal{S}}_i. \tag{3.7}$$

By substituting (2.13) into (3.7), one has

$$\dot{\mathcal{V}}_1(t) = \sum_{i=1}^{n} \mathcal{S}_i(t) \left(\mathcal{D}^{\gamma} F_i - \bar{\mathcal{K}}_1 \left[|\mathcal{S}_i|^{\mu_1} sgn(\mathcal{S}_i) \right] - \bar{\mathcal{K}}_2 \left[|\mathcal{S}_i|^{\mu_2} sgn(\mathcal{S}_i) \right] \right). \tag{3.8}$$

Using (2.15), one obtains (3.8) as follows:

$$\dot{\mathcal{V}}_1(t) \leq -\bar{\mathcal{K}}_1 \sum_{i=1}^{n} |\mathcal{S}_i|^{\mu_1+1} - \bar{\mathcal{K}}_2 \sum_{i=1}^{n} |\mathcal{S}_i|^{\mu_2+1} + \Xi \|\mathcal{S}\|. \tag{3.9}$$

Then (3.9) can be rewritten as

$$\dot{\mathcal{V}}_1(t) \leq -\bar{\mathcal{K}}_1 \sum_{i=1}^{n} \left(|\mathcal{S}_i|^2 \right)^{\frac{\mu_1+1}{2}} - \bar{\mathcal{K}}_2 \sum_{i=1}^{n} \left(|\mathcal{S}_i|^2 \right)^{\frac{\mu_2+1}{2}} + \urcorner, \tag{3.10}$$

where $\urcorner = \Xi \|\mathcal{S}\|$. Using Lemma 3, one can compute that

$$\dot{\mathcal{V}}_1(t) \leq -\bar{\mathcal{K}}_1 \left(\sum_{i=1}^{n} |\mathcal{S}_i|^2 \right)^{\frac{\mu_1+1}{2}} - \bar{\mathcal{K}}_2 n^{\frac{1-\mu_2}{2}} \left(\sum_{i=1}^{n} |\mathcal{S}_i|^2 \right)^{\frac{\mu_2+1}{2}} + \urcorner. \tag{3.11}$$

Equation (3.11) can be expressed as follows:

$$\dot{\mathcal{V}}_1(t) \leq -\bar{\mathcal{K}}_1 2 \mathcal{V}_1^{\frac{\mu_1+1}{2}} - \bar{\mathcal{K}}_2 n^{\frac{1-\mu_2}{2}} 2 \mathcal{V}_1^{\frac{\mu_2+1}{2}} + \urcorner, \tag{3.12}$$

$$\dot{\mathcal{V}}_1(t) \leq -\bar{\mathcal{K}}_1 2^{\frac{\mu_1+1}{2}} \mathcal{V}_1^{\frac{\mu_1+1}{2}} - \bar{\mathcal{K}}_2 n^{\frac{1-\mu_2}{2}} 2^{\frac{\mu_2+1}{2}} \mathcal{V}_1^{\frac{\mu_2+1}{2}} + \urcorner. \tag{3.13}$$

Lemma 1 states that by choosing appropriate parameters, $\mathcal{S}$ converges in fixed time to a small neighborhood. As a result, the convergence region may be expressed as follows:

$$\mathcal{V}_1 \leq \min\left\{\left(\frac{\urcorner}{k_1(1-\omega)}\right)^{\frac{2}{\mu_1+1}}, \left(\frac{\urcorner}{k_2(1-\omega)}\right)^{\frac{2}{\mu_2+1}}\right\}, \tag{3.14}$$

where $k_1 = \bar{\mathcal{K}}_1 2^{\frac{\mu_1+1}{2}}, k_2 = \bar{\mathcal{K}}_2 n^{\frac{1-\mu_2}{2}} 2^{\frac{\mu_2+1}{2}}$, $0 < \omega < 1$. And, the settling time can be formulated as follows:

$$T_1 \leq \frac{2}{k_1\omega(1-\mu_1)} + \frac{2}{k_2\omega(\mu_2-1)}. \tag{3.15}$$

Now, stability of the tracking error will be investigated. Therefore, if sliding manifold (2.5) goes to near zero ($\mathcal{S} \equiv 0$), e achieves stability in fixed time as follows:

$$\mathcal{D}^{\gamma} e = -\mathcal{K}_1 \mathcal{D}^{\gamma-1}\left[|e|^{\lambda_1} sign(e)\right] - \mathcal{K}_2 \mathcal{D}^{\gamma-1}\left[|e|^{\lambda_2} sign(e)\right].$$

Theorem 2. The sliding mode has the stable dynamics described by (2.5), with its state trajectories tending to zero in a fixed amount of time.

Proof. The suitable Lyapunov candidate can be selected as

$$\mathcal{V}_2 = \frac{1}{2}\sum_{i=1}^{n} e_i^2. \tag{3.16}$$

This can further be derived as follows:

$$\dot{\mathcal{V}}_2 = \sum_{i=1}^{n} e_i \dot{e}_i = \sum_{i=1}^{n} e_i \mathcal{D}^{1-\gamma}(\mathcal{D}^{\gamma} e_i). \tag{3.17}$$

By substituting $\mathcal{D}^{\gamma} e$ into (3.17), we can obtain

$$\dot{\mathcal{V}}_2 = \sum_{i=1}^{n} e_i \mathcal{D}^{1-\gamma}\left(-\mathcal{K}_1 \mathcal{D}^{\gamma-1}\left[|e|^{\lambda_1} sign(e)\right] - \mathcal{K}_2 \mathcal{D}^{\gamma-1}\left[|e|^{\lambda_2} sign(e)\right]\right). \tag{3.18}$$

Simplification of (3.18) yields

$$\dot{\mathcal{V}}_2 = \sum_{i=1}^{n} e_i \left(-\mathcal{K}_1\left[|e|^{\lambda_1} sign(e)\right] - \mathcal{K}_2\left[|e|^{\lambda_2} sign(e)\right]\right). \tag{3.19}$$

Equation (3.19) is given as

$$\dot{\mathcal{V}}_2 = -\mathcal{K}_1 \sum_{i=1}^{n} |e|^{\lambda_1+1} - \mathcal{K}_2 \sum_{i=1}^{n} |e|^{\lambda_2+1}. \tag{3.20}$$

Equation (3.20) can be rewritten as

$$\dot{\mathcal{V}}_2 = -\mathcal{K}_1 \sum_{i=1}^{n} \left(|e|^2\right)^{\frac{\lambda_1+1}{2}} - \mathcal{K}_2 \sum_{i=1}^{n} \left(|e|^2\right)^{\frac{\lambda_2+1}{2}}. \tag{3.21}$$

Using Lemma 3, (3.21) can be obtained as follows:

$$\dot{\mathcal{V}}_2 \leq -\mathcal{K}_1\left(\sum_{i=1}^{n}|e|^2\right)^{\frac{\lambda_1+1}{2}} - \mathcal{K}_2 n^{\frac{1-\lambda_2}{2}}\left(\sum_{i=1}^{n}|e|^2\right)^{\frac{\lambda_2+1}{2}}. \tag{3.22}$$

Then (3.22) can be given as

$$\dot{\mathcal{V}}_2 \leq -\mathcal{K}_1(2\mathcal{V}_2)^{\frac{\lambda_1+1}{2}} - \mathcal{K}_2 n^{\frac{1-\lambda_2}{2}}(2\mathcal{V}_2)^{\frac{\lambda_2+1}{2}}. \tag{3.23}$$

Simplification of (3.23) yields

$$\dot{\mathcal{V}}_2 \leq -\mathcal{K}_1 2^{\frac{\lambda_1+1}{2}}\mathcal{V}_2^{\frac{\lambda_1+1}{2}} - \mathcal{K}_2 n^{\frac{1-\lambda_2}{2}} 2^{\frac{\lambda_2+1}{2}}\mathcal{V}_2^{\frac{\lambda_2+1}{2}}. \tag{3.24}$$

With Lemma 2, the fixed settling time can be computed as follows:

$$T_2 \leq \frac{1}{\tilde{K}_1(1-\frac{\lambda_1+1}{2})} + \frac{1}{\tilde{K}_2(\frac{\lambda_2+1}{2}-1)}, \tag{3.25}$$

where

$$\tilde{K}_1 = \mathcal{K}_1 2^{\frac{\lambda_1+1}{2}},\ \tilde{K}_2 = \mathcal{K}_2 n^{\frac{1-\lambda_2}{2}} 2^{\frac{\lambda_2+1}{2}}.$$

Hence, the state trajectories tend toward zero in a fixed time interval.

For the stability analysis of the error dynamics, the selected Lyapunov candidate is given as

$$\mathcal{V}_3 = \frac{1}{2}\sum_{i=1}^{n}\varepsilon_i^2. \tag{3.26}$$

Then its derivative is computed as follows:

$$\dot{\mathcal{V}}_3 = \sum_{i=1}^{n}\varepsilon_i\dot{\varepsilon}_i. \tag{3.27}$$

Substitution of $\dot{\varepsilon}$ yields

$$\dot{\mathcal{V}}_3 = \sum_{i=1}^{n}\varepsilon_i\left(-\kappa_1|\varepsilon|^{\varsigma_1}sign(\varepsilon) - \kappa_2|\varepsilon|^{\varsigma_2}sign(\varepsilon)\right). \tag{3.28}$$

Equation (3.28) can be simplified to obtain

$$\dot{\mathcal{V}}_3 = -\kappa_1\sum_{i=1}^{n}|\varepsilon|^{\varsigma_1+1} - \kappa_2\sum_{i=1}^{n}|\varepsilon|^{\varsigma_2+1}. \tag{3.29}$$

Then, (3.29) is obtained as follows:

$$\dot{\mathcal{V}}_3 = -\kappa_1\sum_{i=1}^{n}\left(|\varepsilon|^2\right)^{\frac{\varsigma_1+1}{2}} - \kappa_2\sum_{i=1}^{n}\left(|\varepsilon|^2\right)^{\frac{\varsigma_2+1}{2}}. \tag{3.30}$$

Using Lemma 3, we can write

$$\dot{\mathcal{V}}_3 \leq -\kappa_1\left(\sum_{i=1}^{n}|\varepsilon|^2\right)^{\frac{\varsigma_1+1}{2}} - \kappa_2 n^{\frac{1-\varsigma_2}{2}}\left(\sum_{i=1}^{n}|\varepsilon|^2\right)^{\frac{\varsigma_2+1}{2}}. \tag{3.31}$$

Equation (3.31) can be given as

$$\dot{\mathcal{V}}_3 \leq -\kappa_1(2\mathcal{V}_3)^{\frac{\varsigma_1+1}{2}} - \kappa_2 n^{\frac{1-\varsigma_2}{2}}(2\mathcal{V}_3)^{\frac{\varsigma_2+1}{2}}. \tag{3.32}$$

Then, it can be simplified as follows:

$$\dot{\mathcal{V}}_3 \leq -\kappa_1 2^{\frac{\varsigma_1+1}{2}}\mathcal{V}_3^{\frac{\varsigma_1+1}{2}} - \kappa_2 n^{\frac{1-\varsigma_2}{2}}2^{\frac{\varsigma_2+1}{2}}\mathcal{V}_3^{\frac{\varsigma_2+1}{2}}. \tag{3.33}$$

Wtih Lemma 2, the fixed settling time is formulated as follows:

$$T_3 \leq \frac{1}{\bar{K}_1(1-\frac{\varsigma_1+1}{2})} + \frac{1}{\bar{K}_2(\frac{\varsigma_2+1}{2}-1)}, \tag{3.34}$$

where

$$\bar{K}_1 = \kappa_1 2^{\frac{\varsigma_1+1}{2}},$$
$$\bar{K}_2 = \kappa_2 n^{\frac{1-\varsigma_2}{2}}2^{\frac{\varsigma_2+1}{2}}.$$

The settling time convergence can be obtained as T_2, and then e converges to zero. In addition, the ε dynamics are fixed-time stable if $e = 0$ and T_3 exists. Combining T_1, T_2, and T_3, we can obtain the total fixed time convergence as $T = T_1 + T_2 + T_3$. This expression indicates that the system's states will be achieved in a fixed amount of time.

4. Numerical results

Nonlinear two-degree-of-freedom (2-DOF) robotic manipulator dynamics have been utilized to simulate and illustrate the performance of the proposed TDEFxFSMC scheme. To verify and validate the performance of TDEFxFSMC, the proposed findings are compared with the adaptive fixed-time SMC (AFxSMC) [41] and adaptive fractional-order SMC (AFtFoSMC) [42] schemes with and without the uncertain dynamics. The uncertain 2-DOF manipulators are considered unknown with outside disturbances. The system dynamics of a 2-DOF robotic manipulator are provided as follows:

$$\mathfrak{m}(q) = \begin{bmatrix} \mathfrak{m}_{11} & \mathfrak{m}_{12} \\ \mathfrak{m}_{21} & \mathfrak{m}_{22} \end{bmatrix}, \mathfrak{c}(q,\dot{q})\dot{q} = \begin{bmatrix} \mathfrak{c}_1 \\ \mathfrak{c}_2 \end{bmatrix}, \mathfrak{g}(q) = \begin{bmatrix} \mathfrak{g}_1 \\ \mathfrak{g}_2 \end{bmatrix}, \ \mathfrak{u} = \begin{bmatrix} \mathfrak{u}_1 \\ \mathfrak{u}_2 \end{bmatrix},$$

$$q_d = \begin{bmatrix} 0.35e^{-4t} - 1.4e^{-t} + 1.25 \\ -0.25e^{-4t}e^{-t} + 1.25 \end{bmatrix}, \mathfrak{d}(t) = \begin{bmatrix} 0.5\sin(\dot{q}_1) \\ 1.1\sin(\dot{q}_2) \end{bmatrix},$$

$$\mathfrak{f}(t) = \begin{bmatrix} 1.5\dot{q}_1 + 0.5\sin(1.5q_1) \\ 1.3\dot{q}_2 + 0.8\sin(2q_2) \end{bmatrix},$$

where

$$\mathfrak{m}_{11} = (\mathfrak{m}_1 + \mathfrak{m}_2)l_1^2 + \mathfrak{m}_2(l_2^2) + 2\cos(q_2)\mathfrak{m}_2 l_1 l_2 + I_2,$$

$$\mathfrak{m}_{12} = \mathfrak{m}_2 l_2^2 + \cos(q_2)\mathfrak{m}_2 l_1 l_2, \quad \mathfrak{m}_{21} = \mathfrak{m}_{12}, \quad \mathfrak{m}_{22} = \mathfrak{m}_2 l_2^2 + I_1,$$

$$\mathfrak{c}_1 = -\sin(q_2)\mathfrak{m}_2 l_2 l_1 \dot{q}_1 \dot{q}_1 - 2\sin(q_2)\mathfrak{m}_2 l_2 l_1 \dot{q}_1 \dot{q}_2, \quad \mathfrak{c}_2 = \sin(q_2)\mathfrak{m}_2 l_2 l_1 \dot{q}_2 \dot{q}_2,$$

$$\mathfrak{g}_1 = \cos(q_1)(\mathfrak{m}_1 l_1 + \mathfrak{m}_2 l_2)\mathfrak{g} + \cos(q_1 + q_2)\mathfrak{m}_2 l_2 \mathfrak{g}, \quad \mathfrak{g}_2 = \cos(q_1 + q_2)\mathfrak{m}_2 l_2 \mathfrak{g}.$$

The robot parameters are as follows: lengths $l_1 = 1\,m$, $l_2 = 1\,m$, the masses $\mathfrak{m}_1 = 0.15\,kg$, $\mathfrak{m}_2 = 0.15\,kg$, the moment of inertia $I_1 = I_2 = 0.5\ kg.m^2$, and the gravity constant $\mathfrak{g} = 9.8\ m/s^2$. The diagram of the 2-DOF manipulator is shown in Figure 2.

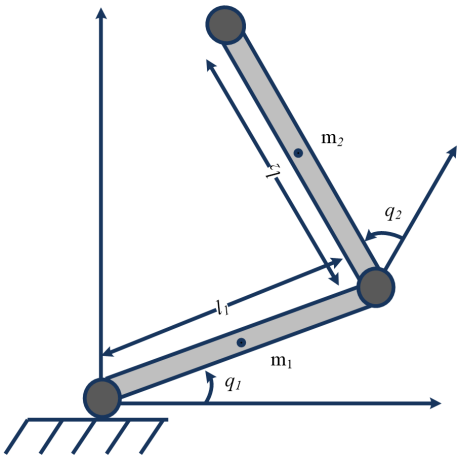

Figure 2. Two-*DOF* robotic manipulator system.

The suitable parameters of the proposed TDEFxFSMC scheme (2.9) were chosen as $\varsigma_1 = 0.7$, $\varsigma_2 = 1.1$, $\lambda_1 = 0.7$, $\lambda_2 = 1.1$, $\mu_1 = 0.9$, $\mu_2 = 1.1$, $\mathcal{K}_1 = 0.09$, $\mathcal{K}_2 = 0.09$, $\bar{\mathcal{K}}_1 = 30.5$, $\bar{\mathcal{K}}_2 = 30.5$, $\kappa_1 = 5.05$, $\kappa_2 = 10.3$, $\alpha = 0.6$, and the fractional value $\gamma = 0.01$. Moreover, the initial values were set as $q_1(0) = 2.1$, $q_2(0) = 0.3$, and the constant time delay was $z = 0.0001$.

4.1. Proposed scheme for nominal system

In order to compare the suggested approach with AFxSMC and AFtFoSMC for the nominal system, we applied the three schemes and obtained the simulation results for joint position tracking as in Figures 3 and 4, tracking errors as in Figures 5 and 6, and control torques as in Figures 7 and 8.

The findings for the nominal system of the robotic manipulator conclusively demonstrate the enhanced tracking efficacy of the suggested approach with swift convergence, a steady-state response, and chatter-free control inputs.

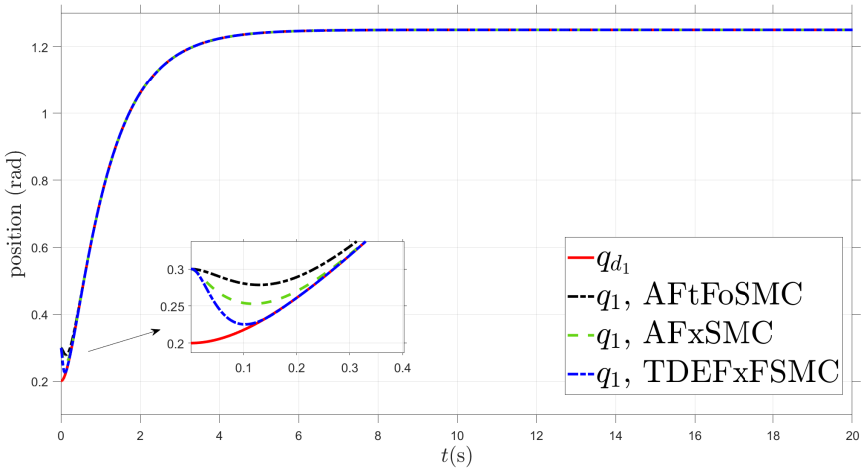

Figure 3. Joint position q_1.

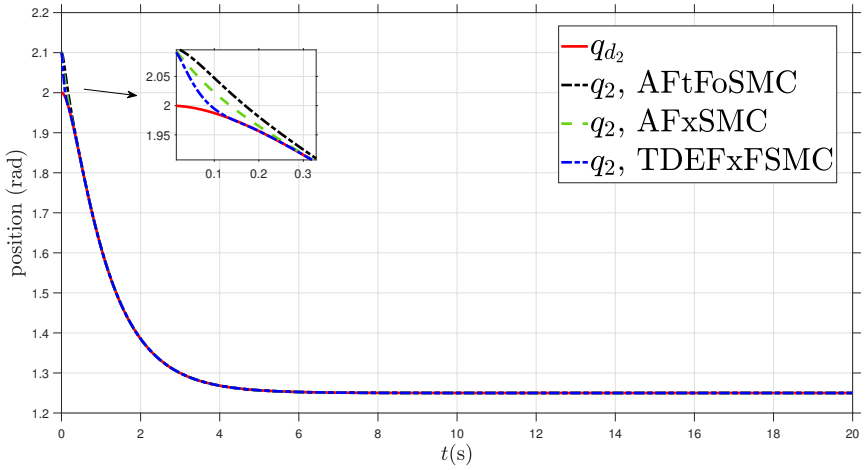

Figure 4. Joint position q_2.

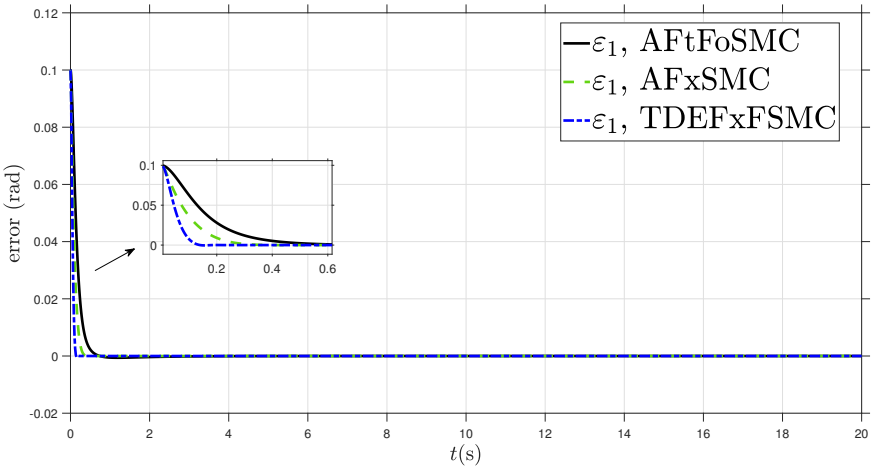

Figure 5. Tracking error ε_1.

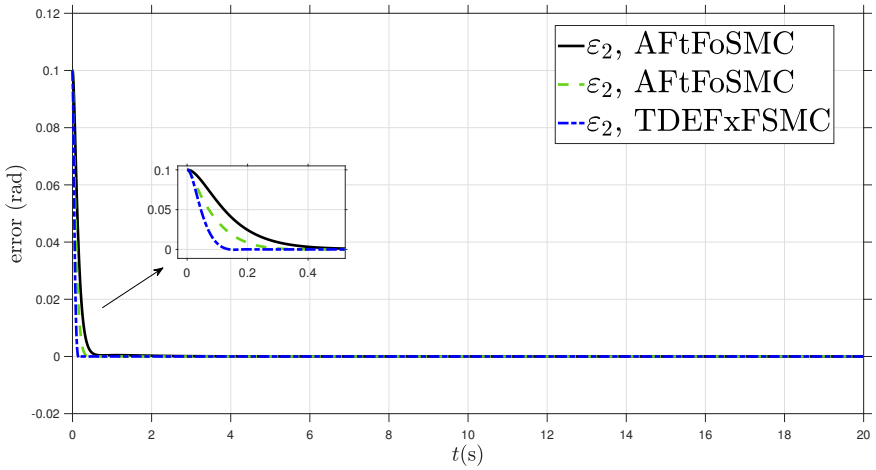

Figure 6. Tracking error ε_2.

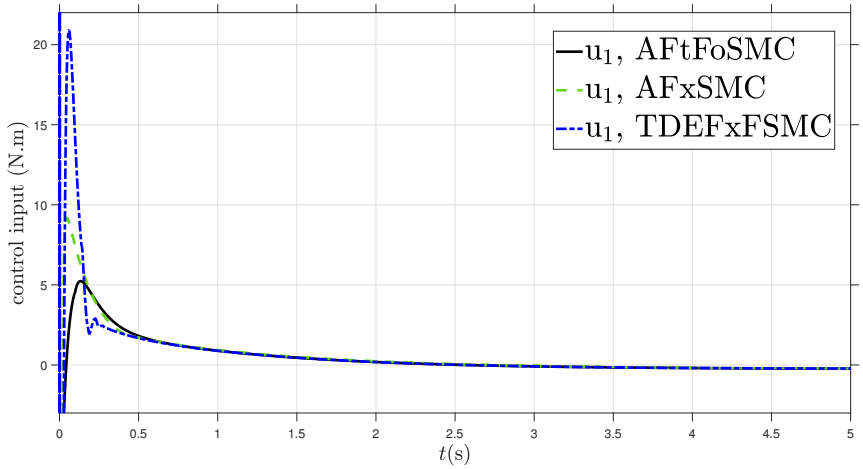

Figure 7. Control input u_1.

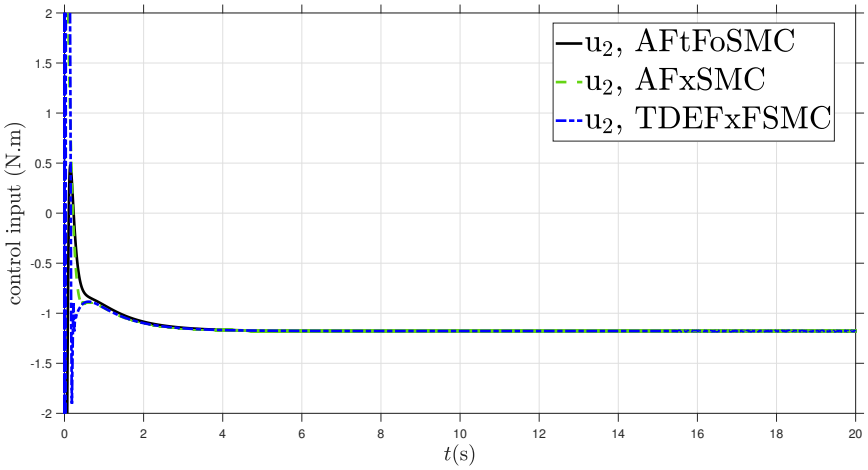

Figure 8. Control input u_2.

4.2. Proposed scheme for system under uncertainties and disturbances

In this instance, comparisons between the suggested approach with AFxSMC and AFtFoSMC under various disturbances and uncertainties are demonstrated here. Therefore, Figures 9–14 show the comparable analyses of tracking errors, position tracking, and control torque under uncertainties and disturbances. Based on the resulting simulations, Figures 9–12 show that the joint position of the robotic manipulator accurately tracks the planned trajectory. Furthermore, the suggested method's good chatter-free control input performance is demonstrated in Figures 13 and 14. Therefore, the performance of the compared method is acceptable without uncertainties and disturbances. Moreover, the estimation of the unknown dynamics of the robotic manipulator are given in Figures 15 and 16.

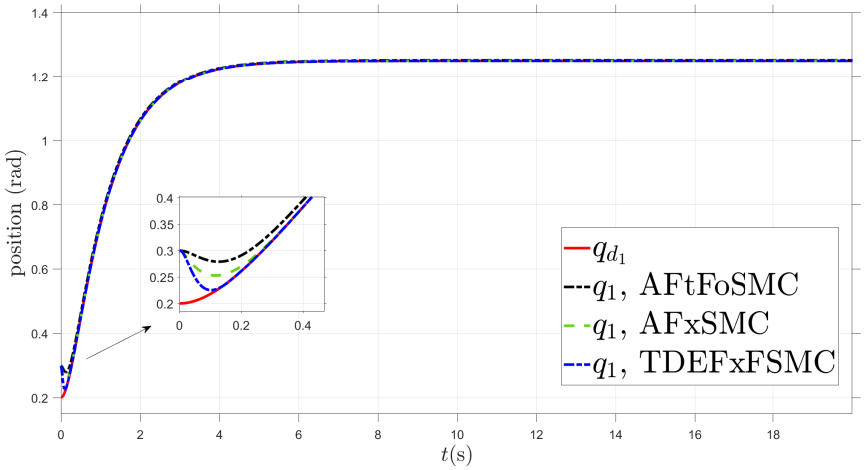

Figure 9. Joint position q_1 with uncertainties and disturbances.

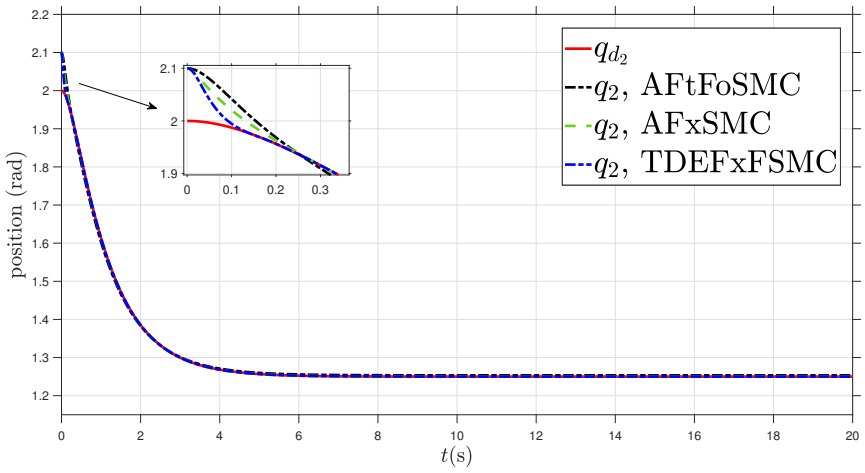

Figure 10. Joint position q_2 with uncertainties and disturbances.

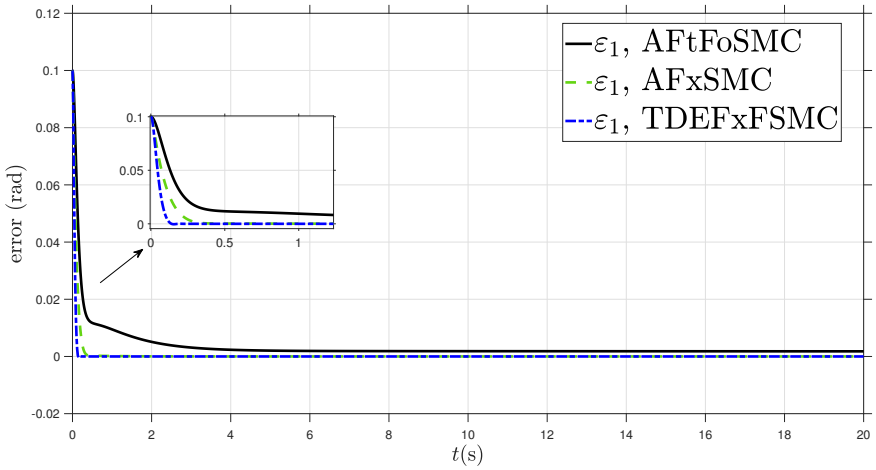

Figure 11. Tracking error ε_1 with uncertainties and disturbances.

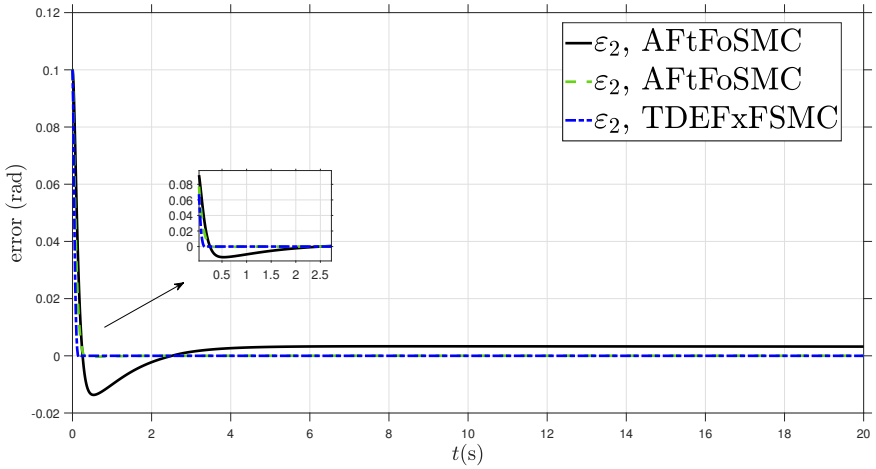

Figure 12. Tracking error ε_2 with uncertainties and disturbances.

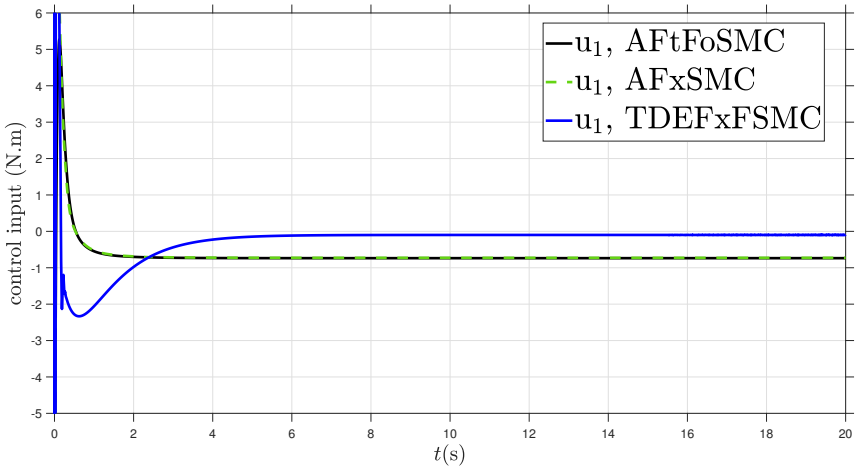

Figure 13. Control inputs u_1 with uncertainties and disturbances.

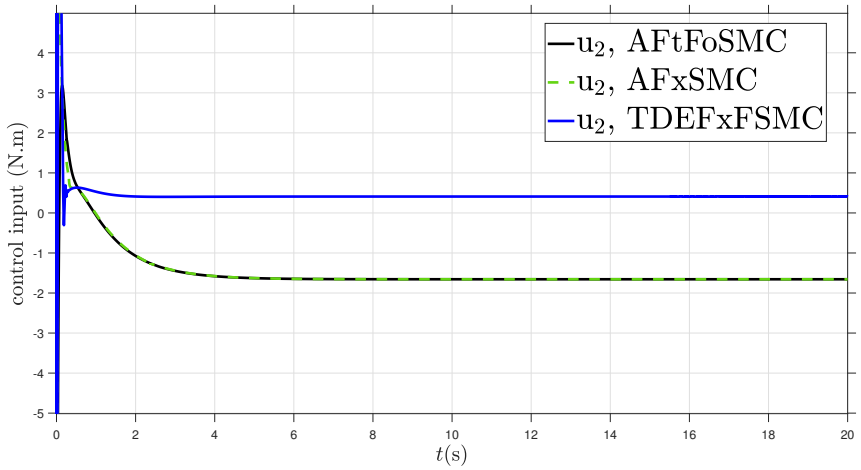

Figure 14. Control inputs u_2 with uncertainties and disturbances.

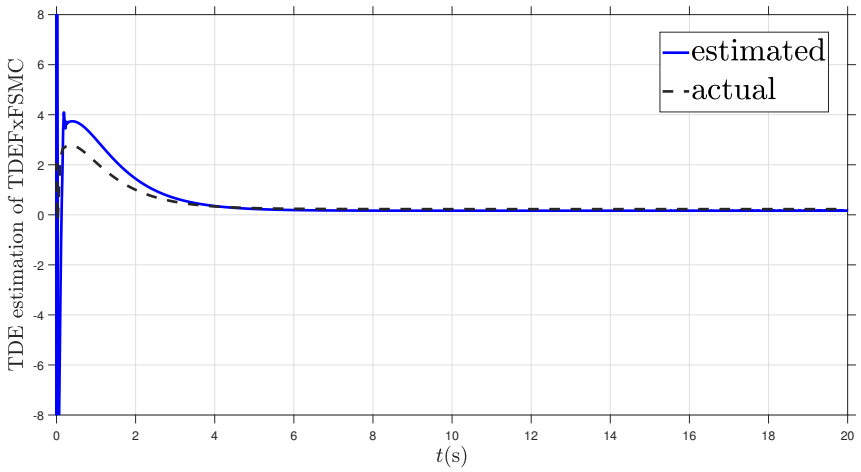

Figure 15. TDE with uncertainties and disturbances, actual ($\mathfrak{Y}_1$) and estimated ($\hat{\mathfrak{Y}}_1$).

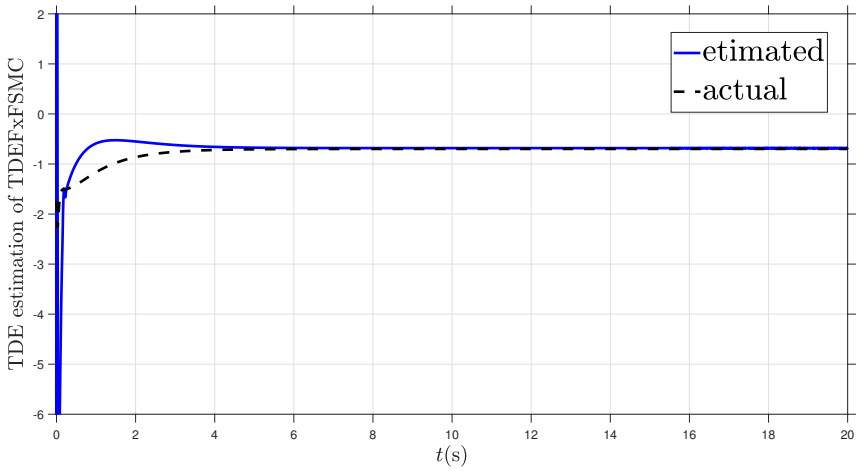

Figure 16. TDE with uncertainties and disturbances, actual ($\mathfrak{Y}_2$) and estimated ($\hat{\mathfrak{Y}}_2$).

Figures 7–10 demonstrate how the dynamics of a robotic manipulator are significantly affected by uncertainty and external disturbances. On the other hand, the findings clearly demonstrate that the suggested strategy achieves effective tracking and quick convergence capabilities while firmly suppressing the effect of uncertain dynamics. For further analyses, the root mean square (RMS) errors of the TDEFxFSMC scheme were calculated to be $\varepsilon_{1_{RMS}} = 0.0042$ and $\varepsilon_{2_{RMS}} = 0.0041$, RMS errors of the AFxSMC method were determined to be $e_{1_{RMS}} = 0.0052$ and $e_{2_{RMS}} = 0.0051$, and RMS errors of the AFtFoSMC method were calculated to be $\tilde{q}_{1_{RMS}} = 0.0070$ and $\tilde{q}_{2_{RMS}} = 0.0068$. Hence, the simulated results and the quantitative outcomes show that the TDEFxFSMC scheme yields better performance.

5. Discussion

In this section, we discuss the results of comparing the proposed TDEFxFSMC scheme, the AFxSMC method, and the AFtFoSMC method in detail. In addition, the limitations of the proposed method parameters are discussed extensively.

It is clear from the simulation findings in Section 4 that, even in the presence of uncertainty and outside disturbance, the recommended approach is model-free and robust against the unknown unmodeled dynamics. Better position tracking, rapid convergence, and non-chatter control inputs were observed in the simulations for the proposed TDEFxFSMC scheme. Additionally, these outcomes have been attained by using appropriate parameters like $\bar{\mathcal{K}}_i$, κ_i, and $\mathcal{K}_i$. Furthermore, the fixed time was set to be dependent on other factors, including $\bar{\mathcal{K}}_i$, μ_i, ϖ, $\mathcal{K}_i$, λ_i, κ_i, and ς_i. By choosing the right parameters, it is possible to achieve fixed-time stability.

Excellent performance was achieved via the TDEFxFSMC technique for the unknown uncertain robot dynamics. This has been demonstrated by its improved tracking performance, fast convergence speed, and non-chatter inputs. In addition, the appropriate values for the suggested approach were determined to be within ranges like $\mathcal{K}_i > 0$, $\bar{\mathcal{K}}_i > 0$, $\kappa_i > 0$, $0 < \varsigma_1, \lambda_1, \mu_1 < 1$, and $\varsigma_2, \lambda_2, \mu_2 > 1$. Therefore, if these parameters are not selected within the given ranges, the fixed-time stability will not be maintained in closed-loop dynamics. The results of (3.15), (3.25), and (3.34) respectively make it clear that T_1, T_2 and T_3 are inversely related to $\bar{\mathcal{K}}_i$, $\mathcal{K}_i$ and κ_i. However, $\mathcal{K}_i$, κ_i and $\bar{\mathcal{K}}_i$ are proportional to $\mathfrak{u}(t)$ in (2.9). Thus, in order to achieve both closed-loop system stability and fixed-time convergence simultaneously, the proper amount of $\bar{\mathcal{K}}_i$, κ_i, and $\mathcal{K}_i$ must be appropriately selected. Additionally, since the other parameters' ranges are known such μ_i, ς_i and λ_i, it is feasible to select suitable values by using an appropriate approach.

6. Conclusions

Controlling the unknown nonlinear robotic dynamics with external disturbances and uncertainties is the primary objective of a TDEFxFSMC. The unknown nonlinear robotic dynamics are estimated via the TDE technique. FxSMC is used to achieve strong fixed-time error convergence performance and stability. Additionally, fractional-order methodology has been applied to enhance the response of the overall system. The unknown nonlinear dynamics of a 2-DOF robotic system were utilized to demonstrate and verify the effectiveness of the suggested TDEFxFSMC technique. Moreover, the suggested approach has been compared with AFxSMC and AFtFoSMC. The simulation results demonstrate the effectiveness of the proposed TDEFxFSMC scheme, which provides fast convergence,

low position error, smooth control input, and the capacity to estimate unknown nonlinear robotic dynamics.

Use of AI tools declaration

The authors declare they have not used Artificial Intelligence (AI) tools in the creation of this article.

Acknowledgments

The authors would like to thank Prince Sultan University, Riyadh, Saudi Arabia for supporting this work. This research is supported by Automated Systems and Soft Computing Lab (ASSCL), Prince Sultan University, Riyadh, Saudi Arabia.

Conflict of interest

All authors declare no conflicts of interest that may influence the publication of this paper.

References

1. A. T. Azar, Q. Zhu, A. Khamis, D. Zhao, Control design approaches for parallel robot manipulators: a review, *Int. J. Model. Identif. Control*, **28** (2017), 199–211. https://doi.org/10.1504/IJMIC.2017.086563
2. K. K. Ayten, M. H. Çiplak, A. Dumlu, Implementation a fractional-order adaptive model-based PID-type sliding mode speed control for wheeled mobile robot, *Proceedings of the Institution of Mechanical Engineers, Part I: Journal of Systems and Control Engineering*, **233** (2019), 1067–1084. https://doi.org/10.1177/0959651819847395
3. M. S. Zanjani, S. Mobayen, Event-triggered global sliding mode controller design for anti-sway control of offshore container cranes, *Ocean Eng.*, **268** (2023), 113472. https://doi.org/10.1016/j.oceaneng.2022.113472
4. M. Bakouri, A. Alqarni, S. Alanazi, A. Alassaf, I. AlMohimeed, M. A. Aboamer, et al., Robust dynamic control algorithm for uncertain powered wheelchairs based on sliding neural network approach, *AIMS Math.*, **8** (2023), 26821–26839. https://doi.org/10.3934/math.20231373
5. A. Almasoud, Jamming-aware optimization for UAV trajectory design and internet of things devices clustering, *Complex Intell. Syst.*, **9** (2023), 4571–4590. https://doi.org/10.1007/s40747-023-00970-3
6. S. Ahmed, A. T. Azar, Adaptive fractional tracking control of robotic manipulator using fixed-time method, *Complex Intell. Syst.*, **9** (2023), 369–382. https://doi.org/10.1007/s40747-023-01164-7
7. S. Ahmed, A. T. Azar, M. Tounsi, I. K. Ibraheem, Adaptive control design for Euler-Lagrange systems using fixed-time fractional integral sliding mode scheme, *Fractal Fract.*, **7** (2023), 712. https://doi.org/10.3390/fractalfract7100712
8. S. J. Gambhire, D. R. Kishore, P. S. Londhe, S. N. Pawar, Review of sliding mode based control techniques for control system applications, *Int. J. Dyn. Control*, **9** (2021), 363–378. https://doi.org/10.1007/s40435-020-00638-7

9. H. Yin, B. Meng, Z. Wang, Disturbance observer-based adaptive sliding mode synchronization control for uncertain chaotic systems, *AIMS Math.*, **8** (2023), 23655–23673. https://doi.org/10.3934/math.20231203
10. D. Zhao, S. Li, F. Gao, A new terminal sliding mode control for robotic manipulators, *Int. J. Control*, **82** (2009), 1804–1813. https://doi.org/10.1080/00207170902769928
11. Y. Feng, X. Yu, Z. Man, Non-singular terminal sliding mode control of rigid manipulators, *Automatica*, **38** (2002), 2159–2167. https://doi.org/10.1016/S0005-1098(02)00147-4
12. L. Yang, J. Yang, Nonsingular fast terminal sliding-mode control for nonlinear dynamical systems, *Int. J. Robust Nonlinear Control*, **21** (2011), 1865–1879. https://doi.org/10.1002/rnc.1666
13. C. Ton, C. Petersen, Continuous fixed-time sliding mode control for spacecraft with flexible appendages, *IFAC-PapersOnLine*, **51** (2018), 1–5. https://doi.org/10.1016/j.ifacol.2018.07.079
14. H. Khan, S. Ahmed, J. Alzabut, A. T. Azar, J. F. Gómez-Aguilar, Nonlinear variable order system of multi-point boundary conditions with adaptive finite-time fractional-order sliding mode control, *Int. J. Dyn. Control*, 2024, 1–17. https://doi.org/10.1007/s40435-023-01369-1
15. Y. Su, C. Zheng, P. Mercorelli, Robust approximate fixed-time tracking control for uncertain robot manipulators, *Mech. Syst. Signal Pr.*, **135** (2020), 106379. https://doi.org/10.1016/j.ymssp.2019.106379
16. S. Ahmed, A. T. Azar, I. K. Ibraheem, Nonlinear system controlled using novel adaptive fixed-time SMC, *AIMS Math.*, **9** (2024), 7895–7916. https://doi.org/10.3934/math.2024384
17. Z. Zhu, Z. Duan, H. Qin, Y. Xue, Adaptive neural network fixed-time sliding mode control for trajectory tracking of underwater vehicle, *Ocean Eng.*, **287** (2023), 115864. https://doi.org/10.1016/j.oceaneng.2023.115864
18. Q. D. Nguyen, D. D. Vu, S. C. Huang, V. N. Giap, Fixed-time supper twisting disturbance observer and sliding mode control for a secure communication of fractional-order chaotic systems, *J. Vib. Control*, 2023. https://doi.org/10.1177/10775463231180947
19. I. Podlubny, *Fractional differential equations: an introduction to fractional derivatives, fractional differential equations, to methods of their solution and some of their applications*, Elsevier, 1998.
20. A. Ali, K. Shah, T. Abdeljawad, H. Khan, A. Khan, Study of fractional order pantograph type impulsive antiperiodic boundary value problem, *Adv. Differ. Equ.*, **2020** (2020), 572. https://doi.org/10.1186/s13662-020-03032-x
21. S. Ahmad, A. Ullah, Q. M. Al-Mdallal, H. Khan, K. Shah, A. Khan, Fractional order mathematical modeling of COVID-19 transmission, *Chaos Soliton. Fract.*, **139** (2020), 110256. https://doi.org/10.1016/j.chaos.2020.110256
22. K. Shah, Z. A. Khan, A. Ali, R. Amin, H. Khan, A. Khan, Haar wavelet collocation approach for the solution of fractional order COVID-19 model using Caputo derivative, *Alexandria Eng. J.*, **59** (2020), 3221–3231. https://doi.org/10.1016/j.aej.2020.08.028
23. A. I. Ahmed, M. S. Al-Sharif, M. S. Salim, T. A. Al-Ahmary, Numerical solution of fractional variational and optimal control problems via fractional-order Chelyshkov functions, *AIMS Math.*, **7** (2022), 17418–17443. https://doi.org/10.3934/math.2022960
24. R. Ayad, W. Nouibat, M. Zareb, Y. B. Sebanne, Full control of quadrotor aerial robot using fractional-order FOPID, *Iran. J. Sci. Technol. Trans. Electr. Eng.*, **43** (2019), 349–360. https://doi.org/10.1007/s40998-018-0155-4

25. H. Khan, S. Ahmed, J. Alzabut, A. T. Azar, A generalized coupled system of fractional differential equations with application to finite time sliding mode control for Leukemia therapy, *Chaos Soliton. Fract.*, **174** (2023), 113901. https://doi.org/10.1016/j.chaos.2023.113901
26. T. T. Nguyen, Fractional-order sliding mode controller for the two-link robot arm, *Int. J. Electr. Comput. Eng.*, **10** (2020), 5579–5585. https://doi.org/10.11591/ijece.v10i6.pp5579-5585
27. S. Huang, L. Xiong, J. Wang, P. Li, Z. Wang, M. Ma, Fixed-time fractional-order sliding mode controller for multimachine power systems, *IEEE Trans. Power Syst.*, **36** (2020), 2866–2876. https://doi.org/10.1109/TPWRS.2020.3043891
28. B. D. H. Phuc, V. D. Phung, S. S. You, T. D. Do, Fractional-order sliding mode control synthesis of supercavitating underwater vehicles, *J. Vib. Control*, **26** (2020), 1909–1919. https://doi.org/10.1177/1077546320908412
29. X. Zhang, F. Wu, M. Liu, X. Chen, Fractional-order robust fixed-time sliding mode control for deployment of tethered satellite, *Acta Astronaut.*, **209** (2023), 172–178. https://doi.org/10.1016/j.actaastro.2023.04.041
30. T. C. Lin, T. Y. Lee, V. E. Balas, Adaptive fuzzy sliding mode control for synchronization of uncertain fractional order chaotic systems, *Chaos Soliton. Fract.*, **44** (2011), 791–801. https://doi.org/10.1016/j.chaos.2011.04.005
31. S. Huang, J. Wang, C. Huang, L. Zhou, L. Xiong, J. Liu, et al., A fixed-time fractional-order sliding mode control strategy for power quality enhancement of PMSG wind turbine, *Int. J. Electr. Power Energy Syst.*, **134** (2022), 107354. https://doi.org/10.1016/j.ijepes.2021.107354
32. S. Han, H. Wang, Y. Tian, N. Christov, Time-delay estimation based computed torque control with robust adaptive RBF neural network compensator for a rehabilitation exoskeleton, *ISA Trans.*, **97** (2020), 171–181. https://doi.org/10.1016/j.isatra.2019.07.030
33. A. T. Azar, H. H. Ammar, M. Y. Beb, S. R. Garces, A. Boubakari, Optimal design of PID controller for 2-DOF drawing robot using bat-inspired algorithm, In: A. Hassanien, K. Shaalan, M. Tolba, *Proceedings of the International Conference on Advanced Intelligent Systems and Informatics 2019*, Springer, **1058** (2019), 175–186. https://doi.org/10.1007/978-3-030-31129-2_17
34. M. Van, S. S. Ge, H. Ren, Finite time fault tolerant control for robot manipulators using time delay estimation and continuous nonsingular fast terminal sliding mode control, *IEEE Trans. Cybernetics*, **47** (2016), 1681–1693. https://doi.org/10.1109/TCYB.2016.2555307
35. K. Y. Toumi, O. Ito, A time delay controller for systems with unknown dynamics, *J. Dyn. Sys., Meas., Control*, **112** (1990), 133–142. https://doi.org/10.1115/1.2894130
36. T. C. Hsia, L. S. Gao, Robot manipulator control using decentralized linear time-invariant time-delayed joint controllers, *Proceedings., IEEE International Conference on Robotics and Automation*, IEEE, 1990, 2070–2075. https://doi.org/10.1109/ROBOT.1990.126310
37. S. Ahmed, I. Ghous, F. Mumtaz, TDE based model-free control for rigid robotic manipulators under nonlinear friction, *Sci. Iran.*, 2022. https://doi.org/10.24200/sci.2022.57252.5141
38. Y. Wu, H. Fang, T. Xu, F. Wan, Adaptive neural fixed-time sliding mode control of uncertain robotic manipulators with input saturation and prescribed constraints, *Neural Process. Lett.*, **54** (2022), 3829–3849. https://doi.org/10.1007/s11063-022-10788-8
39. A. Polyakov, Fixed-time stabilization via second order sliding mode control, *IFAC Proc. Vol.*, **45** (2012), 254–258. https://doi.org/10.3182/20120606-3-NL-3011.00109

40. J. Zhai, Z. Li, Fast-exponential sliding mode control of robotic manipulator with super-twisting method, *IEEE Trans. Circuits Syst. II*, **69** (2021), 489–493. https://doi.org/10.1109/TCSII.2021.3081147
41. S. Ahmed, A. T. Azar, M. Tounsi, Adaptive fault tolerant non-singular sliding mode control for robotic manipulators based on fixed-time control law, *Actuators*, **11** (2022), 353. https://doi.org/10.3390/act11120353
42. S. Ahmed, H. Wang, Y. Tian, Fault tolerant control using fractional-order terminal sliding mode control for robotic manipulators, *Stud. Inform. Control*, **27** (2018), 55–64. https://doi.org/10.24846/v27i1y201806

AIMS Press